Postprint

This is the accepted version of a paper presented at *IEEE MTT-S International Microwave Symposium, Philadelphia, USA, 10-15 June 2018.*

N.B. When citing this work, cite the original published paper.

Micromachined Waveguides with Integrated Silicon Absorbers and Attenuators at 220–325 GHz

Bernhard Beuerle, Umer Shah and Joachim Oberhammer

Department of Micro and Nanosystems, KTH Royal Institute of Technology, SE-100 44 Stockholm, Sweden

Abstract—**This paper reports for the first time on micromachined waveguides with integrated micromachined silicon absorbers. In contrast to epoxy-based microwave absorbers, micromachined lossy silicon absorbers are fully compatible with high temperature fabrication and assembly processes for micromachined waveguides. Furthermore, micromachining enables the fabrication of exact, near ideal taper tips for the silicon absorbers, whereas the tip of epoxy-based absorbers cannot be shaped accurately and reproducibly for small waveguides. Silicon of different conductivity is a very well understood and characterized dielectric material, in contrast to conventional absorber materials which are not specified above 60 GHz. Micromachined silicon waveguides with integrated absorbers and attenuators were designed, fabricated and characterized in the frequency band of 220 − 325 GHz. The return and insertion loss for various taper-geometry variations of double-tip tapered absorbers and attenuators was studied. The average return loss for the best investigated device is 19 dB over the whole band. The insertion loss of the two-port attenuators is 16 − 33 dB for different designs and shows an excellent agreement to the simulated results. The best measured devices of the one-port absorbers exhibit an average and worst-case return loss of 22 dB and 14 dB, respectively, over the whole band. The return loss is not characterized by a good simulation-measurement match, which is most likely attributed to placement tolerances of the absorbers in the waveguide cavities affecting the return but not the insertion loss.**

Index Terms—**RF MEMS, micromachined waveguide, rectangular waveguide, submillimeter-wave, terahertz, absorbers, attenuators, matched load**

I. INTRODUCTION

Microwave absorbers and attenuators are extensively used in microwave engineering, in particular for terminating ports of multiport devices with a matched load [1]. For absorbers the main requirements are a high return loss and, especially for integrated systems, a small footprint. The return loss is determined by reflections from the air-to-absorber interface and those from the waveguide backshort, which are attenuated by the absorbing material. In order to keep the former low, different shapes, in particular tapered geometries, are widely employed [2] [3] [4] [5].

Different absorbing materials are used for wedge-shaped waveguide absorbers, such as conductively loaded epoxy [2] [6] and magnetically loaded epoxides [7] [8]. An epoxy based magnetic castable absorbing material has been characterized in [9] for micromachined waveguides in the frequency band of 220 − 325 GHz and used in [10] and [11] to characterize multiport micromachined couplers and splitters.

However, epoxy-based absorbers are not suitable for harsh environments, in particular elevated temperature. Since the
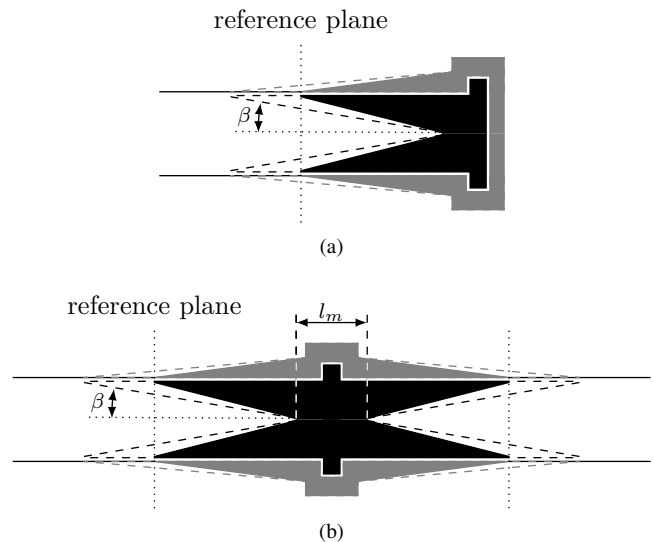

Fig. 1. Schematics of (a) an absorber (black) and (b) an attenuator (black) placed inside a micromachined waveguide cavity with taper angle β and midsection length l_m. The gray area depicts an auxiliary recess around the absorber cavities for easier assembly and to avoid debris.

assembly of micromachined waveguide systems requires chip or wafer bonding at temperatures above 250 °C, such materials can therefore not be utilized in integrated micromachined systems. Furthermore, although smaller in size than traditional microwave absorbers, the footprint of absorbers based on these conventional materials is still quite large due to limited manufacturing possibilities of these plastic materials.

Using silicon as the absorber material offers the advantage of better fabrication tolerances and shape reproducibility provided by proven silicon micromachining techniques. Very

Table I
FABRICATED ABSORBERS (ABx) AND ATTENUATORS (ATy) WITH TAPER ANGLE β AND LENGTH OF THE STRAIGHT ABSORBER MIDSECTION l_m.

device	β (°)	l_m (µm)
AB2	5.43	-
AB3	7.22	-
AB4	10.76	-
AT1	14.22	250
AT2	10.76	250
AT3	8.64	250
AT5	10.76	750
AT7	10.76	1750

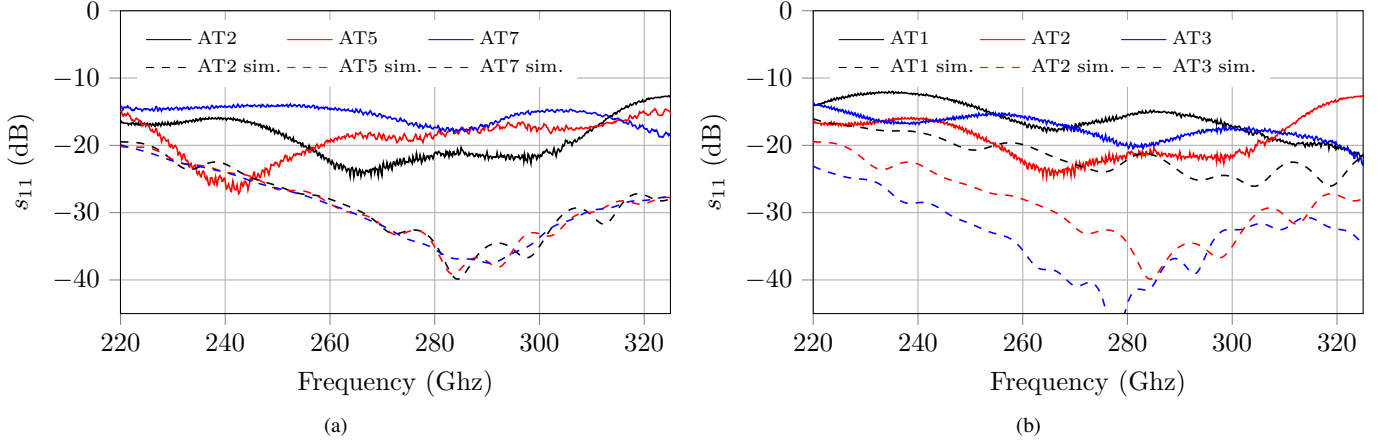Fig. 2. Measured reflection coefficient s_{11} for (a) devices AT2, AT5 and AT7 with the same taper angle $\beta = 10.76°$ and midsection lengths of $l_{m|AT2} = 750\,\mu m$, $l_{m|AT5} = 750\,\mu m$ and $l_{m|AT7} = 1750\,\mu m$ compared to simulations and (b) devices AT1, AT2 and AT3 with a midsection length of $l_m = 250\,\mu m$ and taper angles of $\beta_{AT1} = 14.22°$, $\beta_{AT2} = 10.76°$ and $\beta_{AT3} = 8.64°$ compared to their simulated results.
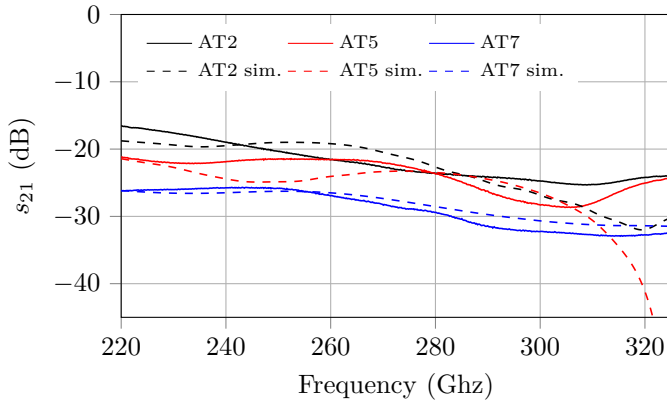

Fig. 3. Measured transmission coefficient s_{21} of the 2-port attenuators with midsections of $l_{m|AT2} = 250\,\mu m$, $l_{m|AT5} = 750\,\mu m$ and $l_{m|AT7} = 1750\,\mu m$, with excellent agreement to the simulated attenuator performance.

recently an optically controlled waveguide attenuator using a thin high resistivity silicon wedge chip in a metal waveguide E-plane split-block configuration utilized silicon as a dielectric absorber [12].

The presented paper investigates and reports for the first time on micromachined silicon absorbers and attenuators integrated into micromachined waveguides implemented for the frequency band of 220 – 325 GHz, and compares various taper geometries.

II. DESIGN AND FABRICATION

The absorbers are fabricated from a $300\,\mu m$ thick standard silicon wafer with a resistivity of $5 – 10\,\Omega$ cm. First the wafer is stripped down to an approximate thickness of $250\,\mu m$ before the absorber structures are fabricated using deep reactive ion etching (DRIE). Due to the inhomogeneity of the stripping process the resulting thickness of the absorbers is in the range of $190 – 250\,\mu m$.

The absorber has a double-tip tapered geometry and is placed in a micromachined waveguide cavity before the wafer/chip thermo-compression bonding (Fig. 1). As the return loss of the absorbers is mainly determined by the taper angle β, absorbers and attenuators with different taper angles are investigated. Additionally the influence of the midsection length l_m (Fig. 1) on the insertion loss of the two-port attenuators is studied. A list of the fabricated designs with the corresponding taper angle β and midsection length l_m is shown in Table I. The micromachined waveguide has a width of $864\,\mu m$ and a reduced height of $275\,\mu m$ as compared to the standard waveguide height [10]. To hold the absorbers accurately in place the cavity has recesses to fit the stub structures of the absorber. The width of the absorbers is slightly smaller than the waveguide width with a clearance of $40\,\mu m$. A scanning electron microscope (SEM) image of the absorber after DRIE is shown in Fig. 4a. For easier assembly and to avoid debris during assembly, an auxiliary recess around the cavity is etched down to $190\,\mu m$ (depicted as the gray area in Fig. 1 and shown in the SEM image Fig. 4b). After the absorber is put into the cavity (Fig. 4c) the waveguide is sealed by thermo-compression bonding with a metallized top chip.

III. CHARACTERIZATION

The absorbers and attenuators are characterized using a Rohde & Schwarz ZVA 24 Vector Network Analyzer with two ZC330 TxRx extension heads over the frequency band of 220 – 325 GHz. A Thru-Reflect-Line (TRL) calibration was performed to move the reference planes to the tips of the absorbers into the micromachined waveguide cavity (dashed lines in Fig. 1).

The measured reflection coefficients s_{11} for attenuators with the same taper angle of $\beta = 10.76°$ are shown in Fig. 2a with the simulated s_{11} as reference. Fig. 2b shows the comparison between the measured and the simulated reflection coefficients for attenuators with the same absorber midsection length $l_m = 250\,\mu m$. Although the measured return loss
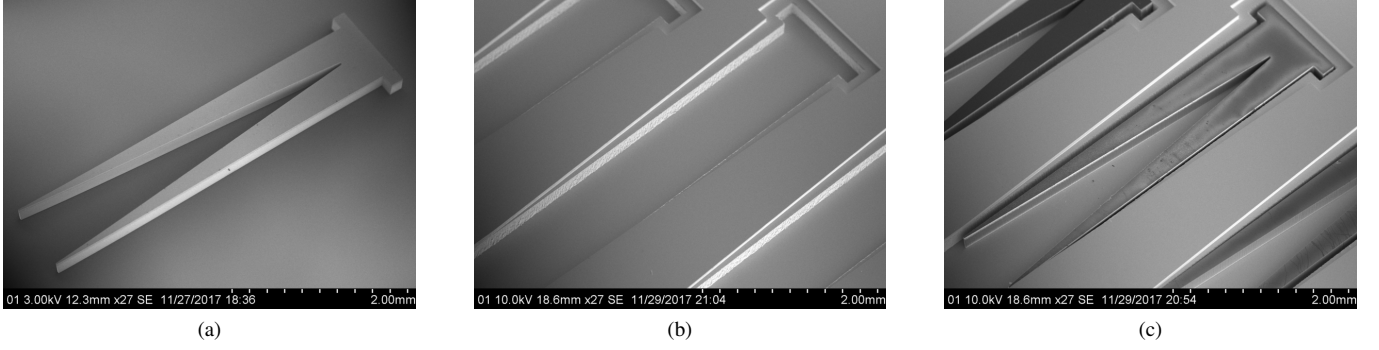
Fig. 4. Scanning Electron Microscope picture of (a) a silicon absorber, (b) an empty absorber waveguide cavity and (c) a waveguide absorber cavity filled with a silicon absorber.
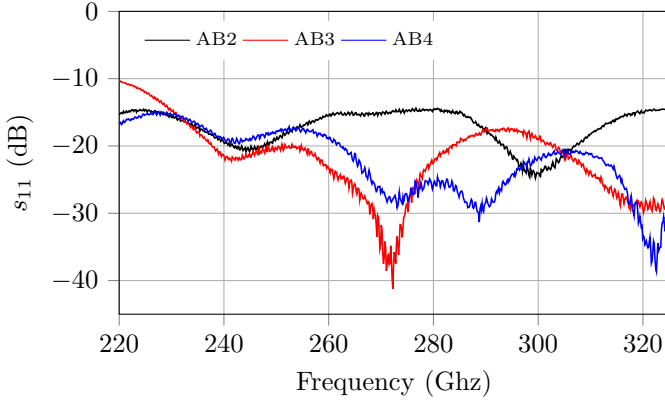

Fig. 5. Measured reflection coefficient s_{11} of the 1-port absorbers with taper angles $\beta_{AB2} = 10.76°$, $\beta_{AB3} = 7.22°$ and $\beta_{AB4} = 5.43°$.

IV. CONCLUSION

This paper presents the first characterization of micromachined and embedded silicon waveguide absorbers and attenuators in the frequency band of $220 - 325\,\mathrm{GHz}$. The influence of different taper angles and midsection lengths of the attenuators on the return and insertion loss was investigated. As the clearance between the silicon absorbers and the waveguide sidewalls influences the correct position of the attenuators in the waveguide and thus the taper angle, no close correlation between the measured and the simulated return loss was established. However, the clearance has no influence on the absorber midsection and thereby the measured insertion loss shows a good match to the simulations.

For the best one-port silicon absorbers, the return loss is better than $14\,\mathrm{dB}$ averaging $22\,\mathrm{dB}$ over the whole band. In addition to their small footprint, this renders them superior to be used as matched loads in integrated systems compared to epoxy based absorbers, which are not compatible to high process temperatures and have inaccurate geometries.

of the devices does not follow the simulated values, the best measured attenuator AT7 achieves an average return loss of $19\,\mathrm{dB}$ in the studied frequency band. The lower measured return loss compared to the simulated one is accredited to the oversized clearance between the silicon attenuators and the waveguide sidewalls.

In Fig. 3 the measured transmission coefficients s_{21} for attenuators with different lengths for the midsection are depicted and show a good match with the simulated values. Whereas the return loss is mainly determined by the taper angle β and thus influenced by the clearance between the attenuator and the waveguide sidewalls, the insertion loss is predominantly defined by the absorber midsection l_m. This can be seen from the close match between the measured transmission coefficient s_{21} and the simulations.

For the one-port absorbers, the reflection coefficient is depicted in Fig. 5. The return loss of the absorbers is higher than $14\,\mathrm{dB}$ averaging $22\,\mathrm{dB}$ for the whole frequency band of $220 - 325\,\mathrm{GHz}$, with the exception of absorber type AB3 having a return loss of $10 - 20\,\mathrm{dB}$ in the lower band of $220 - 230\,\mathrm{GHz}$.

REFERENCES

[1] R. E. Collin, *Foundations for Microwave Engineering.* Institute of Electrical and Electronics Engineers (IEEE), 2001.

[2] E. J. Wollack, D. J. Fixsen, A. Kogut, M. Limon, P. Mirel, and J. Singal, "Radiometric-waveguide calibrators," *IEEE Transactions on Instrumentation and Measurement*, vol. 56, no. 5, pp. 2073–2078, oct 2007.

[3] S. Liu, J. Hu, Y. Zhang, L. Li, W. Zhao, R. Xu, and Q. Xue, "Silicon micromachined waveguide quadrature-hybrid coupler at terahertz frequency band," *Journal of Infrared, Millimeter, and Terahertz Waves*, vol. 36, no. 8, pp. 709–719, may 2015.

[4] S. Liu, J. Hu, Y. Zhang, Y. Liu, T. Ren, R. Xu, and Q. Xue, "Sub-millimeter-wave 10 dB directional coupler based on micromachining technique," *International Journal of Antennas and Propagation*, vol. 2015, pp. 1–8, 2015.

[5] A. Murk, S. Biber, T. Tils, P. Pütz, L.-P. Schmidt, and N. Kämpfer, "Characterization of micromachined waveguide hybrids at 350 and 650 GHz," in *17th International Symposium on Space Terahertz Technology*, May 2006.

[6] E. J. Wollack, D. J. Fixsen, R. Henry, A. Kogut, M. Limon, and P. Mirel, "Electromagnetic and thermal properties of a conductively loaded epoxy," *International Journal of Infrared and Millimeter Waves*, vol. 29, no. 1, pp. 51–61, oct 2007.

[7] A. R. Kerr, H. Moseley, E. Wollack, W. Grammer, G. Reiland, R. Henry, and K. P. Stewart, *MF-112 and MF-116: Compact Waveguide Loads and FTS Measurements at Room Temperature and 5 K*, ALMA, May 2004, ALMA Memo 494.

[8] T. Reck, C. Jung-Kubiak, J. V. Siles, C. Lee, R. Lin, G. Chattopad-hyay, I. Mehdi, and K. Cooper, "A silicon micromachined eight-pixel transceiver array for submillimeter-wave radar," *IEEE Transactions on Terahertz Science and Technology*, vol. 5, no. 2, pp. 197–206, Mar 2015.

[9] B. Beuerle, J. Campion, U. Shah, and J. Oberhammer, "Integrated Micromachined Waveguide Absorbers at 220 – 325 GHz," in *2017 47th European Microwave Conference (EuMC)*, 2017.

[10] J. Svedin, R. Malmqvist, B. Beuerle, U. Shah, and J. Oberhammer, "A 230-300 GHz Low-Loss Micromachined Waveguide Hybrid Coupler," in *2017 47th European Microwave Conference (EuMC)*, 2017.

[11] R. Malmqvist, A. Gustafsson, J. Svedin, B. Beuerle, U. Shah, and J. Oberhammer, "A 220-325 GHz Low-Loss Micromachined Waveguide Power Divider," in *2017 Asia-Pacific Microwave Conference (APMC)*, 2017.

[12] Z. Jiang, M. I. B. Shams, L.-J. Cheng, P. Fay, J. L. Hesler, C.-y. E. Tong, and L. Liu, "Investigation and demonstration of a WR-4.3 optically controlled waveguide attenuator," *IEEE Transactions on Terahertz Science and Technology*, pp. 1–7, 2017.